

Phonon-engineered mobility enhancement in the acoustically mismatched silicon/diamond transistor channels

Denis L. Nika, Evghenii P. Pokatilov, and Alexander A. Balandin^{a)}

Nano-Device Laboratory, Department of Electrical Engineering, University of California-Riverside, Riverside, California 92521, USA

(Received 4 October 2008; accepted 7 October 2008; published online 31 October 2008)

The authors have shown that the low-field electron drift mobility in the ultrathin silicon films can be enhanced if they are embedded within acoustically hard materials such as diamond. The increase results from phonon spectrum modification in the *acoustically mismatched* silicon/diamond heterostructure and suppression of the deformation-potential electron-phonon scattering. The room temperature mobility in silicon films with 2 nm thickness can be increased by a factor of 2–3 depending on the hardness and thickness of the barrier layers. The obtained results suggest a new *phonon-engineering* approach for increasing the speed and drive current of downscaled electronic devices. © 2008 American Institute of Physics. [DOI: 10.1063/1.3007986]

Aggressive scaling of the complementary metal-oxide-semiconductor (CMOS) technology requires a high drive current $I_d \sim C_g \mu$ in order to increase the circuit speed (here C_g is the gate capacitance and μ is the charge carrier mobility). The latter explains very strong motivations for finding new ways for increasing the carrier mobility μ in silicon (Si) transistor channels. There have been a number of methods proposed for the mobility enhancement in the context of CMOS technology.^{1–6} Most methods, including those realized in state-of-the-art CMOS integrated circuits (IC), achieve the electron (hole) mobility enhancement through strain engineering in the lattice mismatched layers. The strain-induced band-structure modification in Si/SiGe films is found to have a strong impact on the carrier mobility and transistor performance.^{1–5} The drive current improvement above ~45% as compared to bulk Si was achieved in the strained-Si n-type metal-oxide-semiconductor field-effect transistors.⁶

At the same time, the strain engineering approach based on utilization of SiGe or other alloy layers has a serious problem related to the thermal budget. It is known that alloys have an order of magnitude smaller thermal conductivity^{7,8} than the constituted bulk semiconductors. The presence of the low thermal-conductivity layer complicates heat escape from the transistor channel down to the substrate heat sink. At the same time, the thermal issues are becoming increasingly important for the high-end electronic chips and the IC performance is now limited by the maximum power, which can be dissipated.⁹ In this letter we show a possibility of the electron mobility enhancement in downscaled Si transistor channels, which is principally different from the conventional technology. Unlike strain engineering our method utilizes materials with high thermal conductivity such as diamond or polycrystalline diamond, which improves heat removal rather than deteriorates it. We show that the phonon-engineering approach, which relies on spatial confinement of acoustic phonon modes, works at room temperature (RT).

We consider a generic heterostructure where a planar Si layer is embedded between two barrier layers made of some

acoustically hard materials. The acoustic hardness is characterized by the acoustic impedance $\eta_{L,T} = \rho V_{L,T}$, where ρ is the mass density and $V_{L,T}$ are the longitudinal or transverse sound velocities. Diamond (either crystalline or polycrystalline) is an example of such material with large $\eta_{L,T}$, which has extremely high thermal conductivity. Although the growth of ultrathin crystalline Si layers on diamond is still a technological challenge the diamond-on-Si and Si-on-diamond structures are already available commercially.¹⁰ It is reasonable to assume that further development of this technology will lead to thin Si layers with diamond claddings and appropriate quality of the interfaces. In the diamond/Si/diamond (D/Si/D) heterostructure the electron (or hole) is confined within Si layer, while the acoustic phonon waves propagate through the whole structure.

If the thickness of Si layer is few nanometers the acoustic phonon spectrum undergoes modification, which is characterized by the appearance of confined dispersion branches similar to electronic minibands.^{11–13} The strength of the modification depends on the mismatch between $\eta_{L,T}$ of the channel and barrier layers. We determined the phonon spectrum using both continuum and atomistic approaches. The continuum approach is better suited for heterostructures with multiple layers but limited to the phonon wave vectors relatively close to the Brillouin zone center (BZC). Owing to the energy and momentum conservation laws, only the BZC phonons participate in the electron-phonon scattering in our structures. For this reason, in the calculation of the electron mobility we used the acoustic phonon spectrum determined by solving the inhomogeneous elasticity equation.^{11–14}

Figures 1(a)–1(d) show the energy dispersions for (a) the “symmetric” acoustic (SA) phonon modes in the freestanding Si slab, (b–c) D/Si/D heterostructures with the different thicknesses of the barrier layer, and (d) Si slab with the clamped-surface boundaries, which correspond to a film embedded in the “absolutely” rigid material. The thickness of the Si layer in all cases is 2 nm to ensure the phonon confinement effect at RT. As one can see from Fig. 1, for all phonon wave vectors q , the energies for each phonon branch s in the freestanding slab are lower than those in the clamped slab. The D/Si/D heterostructures occupy an intermediate position between these two limiting cases depending on the

^{a)} Author to whom correspondence should be addressed. Electronic mail: balandin@ee.ucr.edu. URL: ndl.ee.ucr.edu.

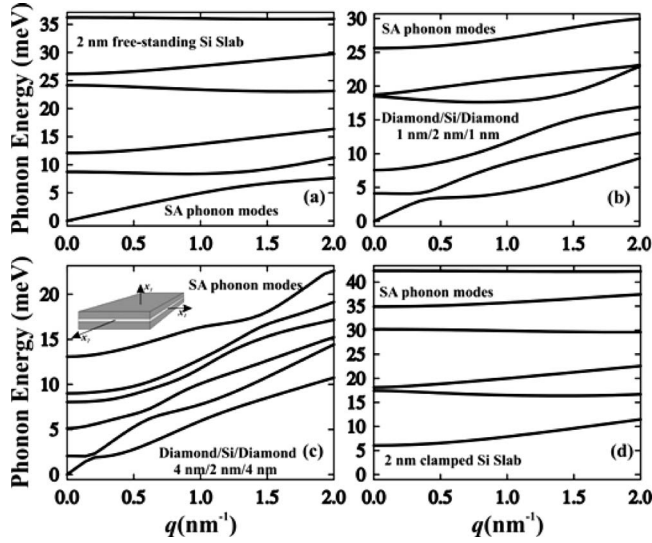


FIG. 1. Dispersion of the SA phonon modes in (a) free-standing Si slab, [(b)–(c)] diamond/Si/diamond heterostructures, and (d) clamped-surface Si slab.

barrier layer thickness. Note that in the lowest phonon branch $s=1$ in the free-standing slab there are always phonons with the infinitesimal energies $\hbar\omega$, for which the Bose phonon distribution $N_{s=1}^f(\hbar\omega) = (e^{\hbar\omega/k_B T} - 1)^{-1} \sim k_B T / \hbar\omega(q) > 1$ for low but finite T (where k_B and \hbar are Boltzmann's and Planck's constant, respectively), while in the clamped-surface slab all phonon modes in the branch $s=1$ are size quantized with the distribution $N_{s=1}^c(\hbar\omega) \sim e^{-\hbar\omega/k_B T} \ll 1$. The SA phonons depicted in Fig. 1 correspond to dilatational acoustic phonons in generic slabs. The “asymmetric” acoustic phonon modes reduce to the flexural acoustic phonons in the slabs. These phonons do not interact with electrons in the ground state and are not considered in this work.¹⁴

We determined the electron spectra in Si slabs and D/Si/D taking into account that the size quantization in the two energy ellipsoids along Z -axis is determined by the heavy electron mass $m_l = 0.98 \times m_0$,¹⁵ while in the four other ellipsoids, with the principal axes in the (X, Y) -plane, the quantization is determined by the light effective mass $m_t = 0.19 \times m_0$,¹⁵ where m_0 is the free electron mass. For Si layer with the thickness $d=2$ nm the electron ground-state energy in the four horizontal ellipsoids $\varepsilon_{\parallel}^0 = 279.94$ meV is larger than the electron ground-state energy $\varepsilon_{\perp}^0 = 87.02$ meV in the two vertical ellipsoids due to the difference between m_l and m_t . This energy splitting leads to larger population of the vertical ellipsoids. The drift electron mobility $\mu(T)$ was calculated using the expression^{16,17}

$$\mu(T) = \frac{e \int_0^{\infty} \varepsilon \tau_1(\varepsilon) f^0(\varepsilon) [1 - f^0(\varepsilon)] d\varepsilon}{m^* k_B T \int_0^{\infty} f^0(\varepsilon_1^0 + \varepsilon) d\varepsilon}, \quad (1)$$

where $f^0(\varepsilon)$ is the Fermi distribution, e is the electron charge, $\tau_1(\varepsilon)$ is the kinetic relaxation time of an electron with energy ε in the first (ground state) electron subband, and ε_1^0 is the size-quantized energy of the electron ground-state subband. The kinetic relaxation times τ_1 have been obtained from the numerical solution of the integral Boltzmann's equation^{17,18}

TABLE I. Material parameters.

| | Si | Diamond |
|-----------------------------------|--------|---------|
| v_L (km/s) | 8.4 | 17.5 |
| v_T (km/s) | 5.84 | 12.8 |
| ρ (g cm ⁻³) | 2.329 | 3.515 |
| η_L (kg cm ⁻² /s) | 1956.4 | 6151.25 |
| η_T (kg cm ⁻² /s) | 1360.1 | 4499.2 |

taking into account the acoustic phonon dispersion, inelasticity of the electron-phonon interaction, and the effect of the electron screening following the procedure outlined in Refs. 19 and 20. We have used the described modeling approach to calculate the electron drift mobility in Si channels embedded between diamond barrier layers and compared it with the results for free-standing and clamped-surface Si slabs. The material parameters used in our calculation are given in Table I.

The dependence of the electron mobility in Si channel on temperature is shown in Fig. 2 for the different thicknesses of the diamond barrier layers. The low-field drift electron mobility in Si channel in the D/Si/D heterostructure is higher than that in free-standing Si slab and increases with the increasing diamond barrier thickness. It is interesting to note that the mobility in the clamped-surface slab is not necessarily the upper limit for the mobility enhancement in Si channels with the acoustically hard barriers. To demonstrate this we calculate the electron mobility in heterostructure with and the acoustically “super hard” (SH) barriers. Under the SH we consider a fictitious material with the elastic modulus three times larger than that in diamond. One can see in Fig. 2 and the inset that there are temperature regions where the electron mobility in SH/Si/SH heterostructure is higher than that in the clamped-surface slabs with the same thicknesses.

The mobility enhancement factor with respect to the mobility in a free-standing Si slab (with the electron sheet density $N_s = 5 \times 10^{12}$ cm⁻²) is in the range 4–10 at low temperature depending on the thicknesses of the acoustically hard barriers. It decreases to the factor of 2–2.5 at RT for 2-nm-thick Si channels. There are several features of the phonon states and electron-phonon interaction in the consid-

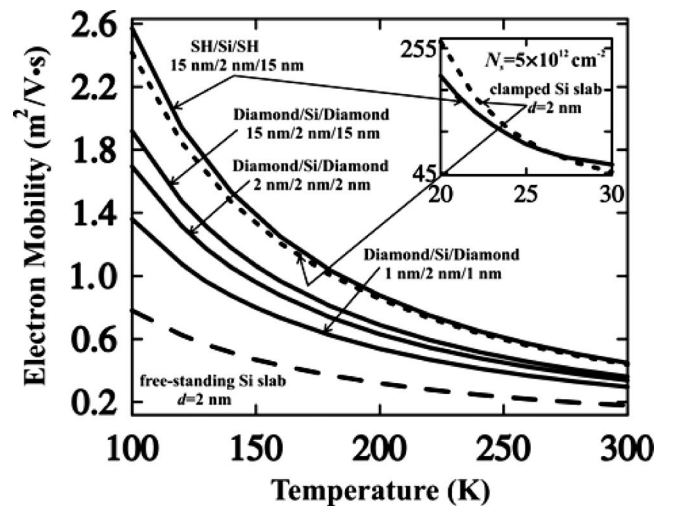


FIG. 2. Electron drift mobility as a function of temperature for 2 nm silicon layers with and without acoustically hard coatings.

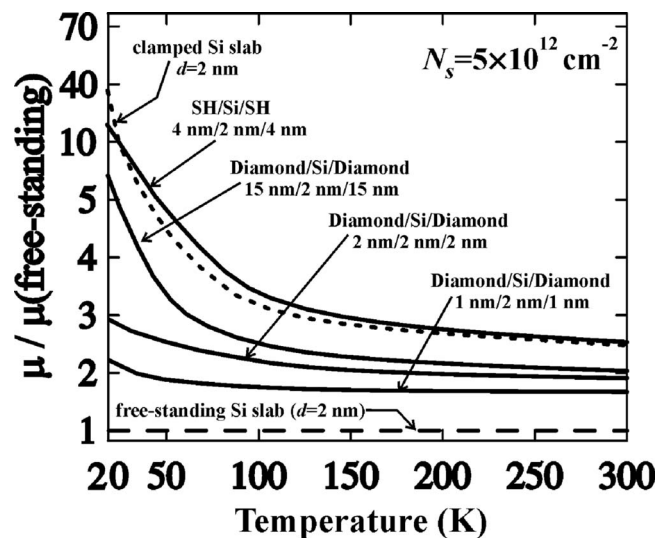


FIG. 3. Mobility enhancement factor as a function of temperature for the electron sheet density $N_s = 5 \times 10^{12} \text{ cm}^{-2}$.

ered heterostructures, which explain the mobility enhancement in Si layers embedded within the acoustically hard barrier layers. As one can deduce from Fig. 1, the phonon density of states (DOS) in the free-standing slab is equal to zero only for $q=0$, while in the clamped-surface slab DOS is equal to zero in the interval of phonon energies up to the first branch ($\sim 5 \text{ meV}$). As a result, the number of phonons available for scattering in the free-standing slab is larger than in the clamped-surface slab for all temperatures. The latter explains a much higher mobility in the clamped-surface slabs, particularly at low temperature. The strength of the electron-phonon deformation potential interaction is smaller for the Si layers embedded within the acoustically hard barriers. It can be explained by suppression of some of the SA modes in D/Si/D heterostructures, where the Si–D interfaces are “fixed” at their positions by the hard diamond barriers. One should note here that the inclusion of the surface roughness scattering does not strongly influence our result obtained for the low-field mobility since the roughness scattering becomes strong for the very high transverse fields only.^{4,5,21} Indeed, even for the very thin, few nanometer thick, Si channels the low-field mobility is limited by the phonons.^{5,21} For convenience of comparison and experimental verification, Fig. 3 shows the mobility enhancement factor with respect to the mobility in a free-standing Si slab. The expected phonon-limited mobility enhancement can reach an order of magnitude at temperature approaching 10 K. The enhancement factor also strongly depends on the acoustic mismatch and the thicknesses of the acoustically hard barriers. It decreases to a

factor of 2–2.5 at RT for 2-nm-thick Si channels. At very low temperatures impurity scattering starts to play the dominant role and has to be taken into account.

In conclusion, we have shown that the RT electron mobility in the ultrathin Si layers can be enhanced if they are embedded within acoustically hard barriers such as diamond. Unlike conventional strain technology the proposed method of the mobility enhancement relies on materials with high thermal conductivity, which is beneficial for thermal management.

This work has been supported by US AFOSR Award No. A9550-08-1-0100 on the electron and phonon engineered nano and heterostructures and by DARPA-SRC FCRP Functional Engineered Nano Architectonics (FENA) Center.

¹Y. Luo and D. K. Nayak, *IEEE Trans. Semicond. Manuf.* **18**, 63 (2005).

²B. Ghyselen, *Mater. Sci. Eng., B* **124–125**, 16 (2005).

³K. Sawano, S. Koh, Y. Shiraki, Y. Hirose, T. Hattori, and K. Nakagawa, *Appl. Phys. Lett.* **82**, 412 (2003); C. W. Leitz, M. T. Currie, M. L. Lee, Z.-Y. Cheng, D. A. Antoniadis, and E. A. Fitzgerald, *J. Appl. Phys.* **92**, 3745 (2002).

⁴C. W. Liu, S. Maikap, and C.-Y. Yu, *IEEE Circuits Devices Mag.* **21**, 21 (2005).

⁵H.-S. P. Wong, *IBM J. Res. Dev.* **46**, 133 (2002).

⁶J.-S. Goo, Q. Xiang, Y. Takamura, H. Wang, J. Pan, F. Arasnia, E. N. Paton, P. Besser, M. V. Sidorov, E. Adem, A. Lochtefeld, G. Braithwaite, M. T. Currie, R. Hammond, M. T. Bulsara, and M.-R. Lin, *IEEE Electron Device Lett.* **24**, 351 (2003).

⁷B. Abeles, *Phys. Rev.* **131**, 1906 (1963).

⁸W. L. Liu and A. A. Balandin, *Appl. Phys. Lett.* **85**, 5230 (2004); *J. Appl. Phys.* **97**, 073710 (2005).

⁹S. P. Gurrum, S. K. Suman, Y. K. Joshi, and A. G. Fedorov, *IEEE Trans. Device Mater. Reliab.* **4**, 709 (2004).

¹⁰See www.sp3inc.com for examples of diamond thin films on Si.

¹¹A. Balandin and K. L. Wang, *Phys. Rev. B* **58**, 1544 (1998).

¹²E. P. Pokatilov, D. L. Nika, and A. A. Balandin, *Superlattices Microstruct.* **33**, 155 (2003).

¹³E. P. Pokatilov, D. Nika, and A. A. Balandin, *Appl. Phys. Lett.* **85**, 825 (2004).

¹⁴E. P. Pokatilov, D. Nika, and A. A. Balandin, *J. Appl. Phys.* **95**, 5626 (2004).

¹⁵See <http://www.ioffe.ru/SVA/NSM/Semicond/Si/bandstr.html#Masses> at the Ioffe Physico-Technical Institute, Russia for accurate values of material parameters.

¹⁶E. P. Pokatilov, D. L. Nika, and A. A. Balandin, *Appl. Phys. Lett.* **89**, 112110 (2006).

¹⁷E. P. Pokatilov, D. L. Nika, and A. A. Balandin, *Appl. Phys. Lett.* **89**, 113508 (2006).

¹⁸N. Bannov, V. Aristov, V. Mitin, and M. A. Stroschio, *Phys. Rev. B* **51**, 9930 (1995).

¹⁹B. K. Ridley, B. E. Foutz, and L. F. Eastman, *Phys. Rev. B* **61**, 16862 (2000).

²⁰D. Zantedo, S. Gokden, N. Balkan, B. K. Ridley, and W. J. Schaff, *Semicond. Sci. Technol.* **19**, 427 (2004).

²¹E. B. Ramayya, D. Vasileska, S. M. Goodnick, and I. Knezevic, *IEEE Trans. Nanotechnol.* **6**, 113 (2007).